Graph Theory Analysis of Functional Connectivity in Major Depression Disorder With High-Density Resting State EEG Data

Shuting Sun, Xiaowei Li, Jing Zhu, Ying Wang, Rong La, Xuemin Zhang, Liuqing Wei, and Bin Hu, *Member, IEEE*

***Abstract*— Existing studies have shown functional brain networks in patients with major depressive disorder (MDD) have abnormal network topology structure. But the methods to construct brain network still exist some issues to be solved. This paper is to explore reliable and robust construction methods of functional brain network using different coupling methods and binarization approaches, based on high-density 128-channel resting state EEG recordings from 16 MDD patients and 16 normal controls (NC). It was found that the combination of imaginary part of coherence and cluster-span threshold outperformed other methods. Based on this combination, right hemisphere function deficiency, symmetry breaking and randomized network structure were found in MDD, which confirmed that MDD had aberrant cognitive processing. Furthermore, clustering coefficient in left central region in theta band and node betweenness centrality in right temporal region in alpha band were significantly negatively correlated with depressive level. And these network metrics had the ability to discriminate MDD from NC, which indicated that these network metrics might be served as the electrophysiological characteristics for probable MDD identification. Hence, this paper may provide reliable methods to construct functional brain network and offer potential biomarkers in MDD.**

***Index Terms*— EEG, major depressive disorder, resting state, functional connectivity, graph theory analysis, network metrics.**

Manuscript received October 22, 2018; revised December 17, 2018; accepted January 17, 2019. Date of publication January 23, 2019; date of current version March 22, 2019. This work was supported in part by the National Basic Research Program of China (973 Program) under Grant 2014CB744600, in part by the National Natural Science Foundation of China under Grant 61632014, Grant 61210010, and Grant 61402211, in part by the International Cooperation Project of Ministry of Science and Technology under Grant 2013DFA11140, in part by the Program of Beijing Municipal Science and Technology Commission under Grant Z171100000117005, and in part by the Fundamental Research Funds for the Central Universities under Grant lzujbky-2017-it74 and Grant lzujbky-2017-it75. *(Corresponding author: Bin Hu.)*

S. Sun, X. Li, J. Zhu, Y. Wang, and R. La are with the Gansu Provincial Key Laboratory of Wearable Computing, School of Information Science and Engineering, Lanzhou University, Lanzhou 730000, China (e-mail: sunsht17@lzu.edu.cn; lixwei@lzu.edu.cn; zhujing@lzu.edu.cn; wangying17@lzu.edu.cn; lar17@lzu.edu.cn).

X. Zhang is with the Beijing Key Laboratory of Applied Experimental Psychology, National Demonstration Center for Experimental Psychology Education, Faculty of Psychology, Beijing Normal University, Beijing 100875, China, also with the State Key Laboratory of Cognitive Neuroscience and Learning and IDG/McGovern Institute for Brain Research, Beijing Normal University, Beijing 100875, China, and also with the Center for Collaboration and Innovation in Brain and Learning Sciences, Beijing Normal University, Beijing 100875, China (e-mail: xmzhang@bnu.edu.cn).

L. Wei is with the Beijing Key Laboratory of Applied Experimental Psychology, National Demonstration Center for Experimental Psychology Education, Faculty of Psychology, Beijing Normal University, Beijing 100875, China (e-mail: weiliuqing1985@126.com).

B. Hu is with the Gansu Provincial Key Laboratory of Wearable Computing, School of Information Science and Engineering, Lanzhou University, Lanzhou 730000, China, also with the CAS Center for Excellence in Brain Science and Intelligence Technology, Shanghai Institutes for Biological Sciences, Chinese Academy of Sciences, Beijing 100864, China, and also with the Beijing Institute for Brain Disorders, Capital Medical University, Beijing 100069, China (e-mail: bh@lzu.edu.cn).

Digital Object Identifier 10.1109/TNSRE.2019.2894423

I. Introduction

MAJOR depressive disorder (MDD) is a globally prevalent psychiatric disorder characterized by persistent low mood, anhedonia and inhibition of thought, cognitive impairment, and even a great suicidal tendency [1], which inflicts psychological and economic burdens on individuals, families and society. With the high prevalence rate of MDD, it is critical to understand the underlying neurophysiological bases of MDD for the effective detection and treatment of this mental disorder.

Within the last decades, investigators have documented that the symptoms of MDD are related to the dysfunction of distributed neuronal network activity across cortical and limbic circuits, rather than to the breakdown of a local specific brain area [2], [3]. Currently, different neurophysiological techniques such as functional Magnetic Resonance Imaging (fMRI), Electroencephalography (EEG) and Magnetoencephalography (MEG) have been extensively adopted to evaluate the brain function connectivity patterns of MDD at resting state [4], [5]. fMRI has a high spatial resolution, while EEG and MEG have high temporal resolution [6]. As we all know, functional connectivity is defined as temporal dependence relationships among the neural signals of spatially separated brain areas [7]. So techniques such as MEG and EEG are the best choice for calculating functional connectivity, especially EEG due to the advantages of high temporal resolution, non-invasive, relative low-cost, portability and practicality, has the potential to act

TABLE I
PREVIOUS STUDIES REPORTING ABNORMALITIES OF RESTING STATE EEG FUNCTIONAL BRAIN NETWORKS IN MDD

Reference	Biotechnology	Subjects	Coupling method	Binarization approach	Reference technique	Results (MDD compared to NC)
[31]	EEG (16 channel electrodes)	12 MDD and 12 NC	Partial directed coherence	threshold	DLM	Larger Kin in the left hemisphere, smaller weighted CC and weighted CPL in the alpha band.
[13]	EEG (30 channel electrodes)	37 MDD and 37 NC	Coherence	Density	DLM	Increased functional connectivity, and decreased CC, CPL and small world in delta, theta, alpha, beta and gamma band.
[10]	EEG (35 channel electrodes)	121 MDD and 37 NC	Coherence	none	through amplitude subtraction into a series of 66 nearest-neighbor bipolar electrode pairs	Increased functional connectivity in delta, theta, alpha and beta frequency band.
[35]	EEG (30 channel electrodes)	10 MDD and 10 NC	Phase Lag Index	threshold	Cz	Decreased CC in beta and delta band, decreased local efficiency in beta band, and increased CPL in alpha band.
[14]	EEG (128 channel electrodes)	23 MDD and 14 NC	Coherence	MST	Cz	Increased functional connectivity and degree fraction in theta band.
[17]	EEG (64 channel electrodes)	13 MDD and 13 NC	Coherence	Density	AVE	Decreased functional connectivity, CPL, local efficiency, CC and rich-club, but increased global efficiency in alpha band.

Note: MDD represents Major Depressive Disorder patients, NC represents Normal Control subjects. MST is Minimum Spanning Tree, AVE is average reference, Cz is vertex electrode, and DLM is digitally linked mastoids. CC represents clustering coefficients, CPL represents characteristic path length, Kin represents in-degree.

as an effective biomarker for identifying the subtle changes of oscillatory activity for MDD [8].

Various coupling methods have been used to obtain the functional connectivity matrices from fMRI, MEG and EEG signals of MDD and other datasets [9], [10]. As the references shown in the Table 1, we find that there are a few researchers study on functional connectivity of MDD at resting state based on sensor layer EEG signals. But the functional connectivity matrices are mainly calculated by coherence (Coh) or correlation (Corr) coupling methods [11]–[14], these methods have been demonstrated will be strongly influenced by the artefacts of volume conduction [15]. To address this issue, researchers [16] have recommended analyzing functional connectivity based on source space instead of sensor space. However, functional brain network assessment of source space still has some problems, for example, there is no unique solution to the inverse problem of mapping from sensor space to source space, and volume conduction effects also exist in the estimated source space. Currently, most electrophysiological studies are analyzed on sensor space, and valuable information can also be obtained by combining sensor space EEG data with advanced coupling methods [17], [18]. So in this paper we will adopt some robust to artifacts of volume conduction methods including imaginary part of coherence (ICoh) [19] and phase lag index (PLI) [20] to calculate functional connectivity matrices based on sensor layer EEG signals of MDD. These methods have been applied to some mental diseases [15], [20], [21], such as Alzheimers disease, Autism spectrum disorders, but are rarely applied to MDD.

In addition, graph theory analysis based on functional connectivity provides important information about topological properties of brain network [22]–[24]. Graph theory analysis has been widely applied to explore the abnormalities of depression in various graph metrics [14], [25], [26], because they are reliable and easy to compute. And brain network can be analyzed in either weighted or binary network. Weighted functional connectivity matrix often contains the spurious connections, which may obfuscate results. So binarizing the weighted connectivity matrix is a more popular approach that not only alleviates the noise level, but also reveals the main topology of the underlying brain activity. Conventionally, binarization approach determines the connection edge exists or not by setting a threshold, which may cause the number of links of functional brain network to be different. Inasmuch as network properties significantly depend on the links number, results will biased to this effect when comparing brain networks with the same threshold. As a binarization method, Density can solve this problem, which keeps the number of links same among all brain networks. Though both of these two approaches have achieved certain success in the study of depression [12], [14], [27], they are arbitrary and subjective. Therefore, in this paper, we will adopt state-of-the-art non-arbitrary unbiased binarization approaches, such as Cluster-Span Threshold (CST) [28], Efficiency Cost Optimization threshold (ECO) [29] and Minimum Spanning Tree (MST) [30], to explore the brain network topology changes of MDD.

According to previous researches, we can find there are two critical issues in the functional brain network of depression that need to be further investigated. First, which coupling method and binarization approach is the most appropriate estimate of true cortical interaction, there is no gold standard. Second, there are inconsistencies in functional connectivity results of MDD. As the references in Table 1, for resting state EEG studies, we find some inconsistent results. Some studies found MDD exhibited decreased characteristic path length (CPL) and clustering coefficient (CC) in different frequency bands [14], [28], but existing study concluded that MDD exhibited increased CPL in alpha band, and decreased CC and local efficiency in beta band [31]. The reason for this difference is that in addition to the impact of subjects and environment, it may be due to the different methods, such as electrode density, reference technique, coupling method and binarization approach. Recent research has shown EEG reference choice had effect on functional connectivity results. And reference electrode standardization technique (REST) significantly reduced the distortion

of connectivity patterns when compared to average reference (AVE), vertex electrode (Cz), and digitally linked mastoids (DLM) [32], moreover, the high-density EEG system could improve topographic accuracy [33]. However, previous studies often used low-density EEG system, such as 16- [34], 30- [12], [31], 35- [11], 64-channels [14] EEG system, and reference methods mainly adopt Cz [13], [31], DLM [12], [34] and AVE [14], to analyze functional brain networks of MDD. So this is the first study to explore reliable functional brain network of MDD using high-density EEG system based on REST reference.

Hence, aiming at aforementioned issues, in this study, we focused on functional brain network analysis of 128-channels high-density resting state EEG signals with REST reference, the EEG data employed was collected from 16 MDD patients and 16 age-, gender- and education-matched NC. The first purpose of this study was by using Coh, ICoh, Corr, PLI and phase lock value (PLV) coupling methods and CST, ECO, MST and Density binarization approaches, to provide a functional connection and network binarization methods that could effectively and reliably identify MDD, and to offer a comparable basis for future research. The second purpose of this study was to further explore alterations in the topology of MDD based on the optimal functional connection and network binarization method, mainly from the following three aspects: we first analyzed characteristic of topology distribution of hubs for MDD patients and healthy subjects; then we studied the symmetry of brain regions based on degree for both of two groups; in the final, we assessed the potential relationships between network properties and clinical state and the classification performance of network measures, we hoped to find out sensitive biomarkers that could be used for probable depression diagnosis.

II. Methods and Materials

A. Subjects

This study involved 32 subjects: 16 patients with MDD (female/male = 7/9, 31.31 ± 10.38 years old, 13.94 ± 3.53 years of education) and 16 NC with no prior or current diagnosis of psychiatric disease (female/male = 7/9, 30.94 ± 9.67 years old, 15.44 ± 3.44 years of education). There were no significant between-group differences in age ($t = 0.106$, $p = 0.917$), or education ($t = -1.217$, $p = 0.233$), or gender ($\chi^2 = 0$, $p = 1$). Patients with MDD were recruited among inpatients and outpatients from Lanzhou University Second Hospital, Gansu, China, diagnosed and recommended by one clinical psychiatrist. The NC were recruited by posters. The study was approved by the Local Research Ethics Committee, and written informed consent was obtained from all subjects before the experiment began. All MDD patients received a structured Mini-International Neuropsychiatric Interview (MINI) [35] that met the diagnostic criteria for major depression of Diagnostic and Statistical Manual of Mental Disorders (DSM) based on the DSM-IV [36]. The inclusion criteria for all participants were the age should between 18 and 55 years old, and primary or higher education level. For MDD patients, the inclusion criteria were the diagnostic criteria of MINI met the criteria for depression, the Patient Health Questionnaire-9item (PHQ-9) [37] score of subjects was greater than or equal to 5, and no psychotropic drug treatment having been performed in the last two weeks. For MDD patients, the exclusion criteria were having mental disorders or brain organ damage, having a serious physical illness, and severe suicidal tendency. For NC, the exclusion criteria included a personal or family history of mental disorders. The exclusion criteria for all subjects were abused or dependent alcohol or psychotropic drugs in the past year, women who were pregnant and in lactation or taking birth control pills. Before the experiment, the self-reported PHQ-9, and Generalized Anxiety Disorder-7 (GAD-7) [38] were self-rated in all subjects. As expected, patients exhibited greater scores in PHQ-9 (MDD: 17.69 ± 3.70, NC: 2.56 ± 2.07), and GAD-7 (MDD: 12.63 ± 5.18, NC: 2.31 ± 1.99) relative to healthy controls ($p < 0.05$). The NC group showed no mood disorder. All participants were rewarded after finishing the experiment.

B. EEG Recording and Preprocessing

For each subject, eye-closed resting state EEG signals were continuously recorded for approximately 5 min using a 128 channel HydroCel Geodesic Sensor Net (HCGSN) with a Cz reference, which were positioned according to the standard international 10/20 system. The sampling frequency was 250 Hz with Net Station acquisition software and Electrical Geodesics amplifiers. Electrode impedance was kept below 50 kΩ [39]. The EEG recordings were further filtered between 0.5 Hz and 40 Hz by a FIR band pass filter and re-referenced against REST [40]. The Net Station waveform tool was used to discard artifacts due to eye movements and muscle activity. Since ocular artifacts (OAs) are presented in the frequency band from 0 to 16 Hz, thus overlapping with the alpha frequency band of 8 - 13 Hz. Therefore we used FastICA to de-noise due to this method has been proved to be effective in delineating overlapping frequency bands [41]. The EEG recordings were continuously divided into 5 s for each segment, the voltage of segments exceeding 150μV were removed. Finally, to ensure that the number of segments is same between subjects, the continuous sixteen valid segments (16 * 5 s = 90 s) without artefacts were selected from each subject for further analysis. In this study, frequency bands of interest were theta (4 - 8 Hz) and alpha (8 - 13 Hz) computed by Hanning Filter, which had been confirmed to make a vital role in identifying depression at resting state [42], [43]. Data processing tool was Matlab R2017a.

C. Construction of Functional Networks

A network consists of nodes and edges between nodes. In this study, each EEG electrode was defined as a node. The edges represented the connectivity strength between different EEG electrodes. To construct functional connectivity matrix, we used 5 coupling methods including Coh, ICoh, Corr, PLI and PLV (a brief description of 5 coupling methods are in the supplementary material-A, NBT toolbox (http://www.nbtwiki.net/) is used in Matlab R2017a). All the

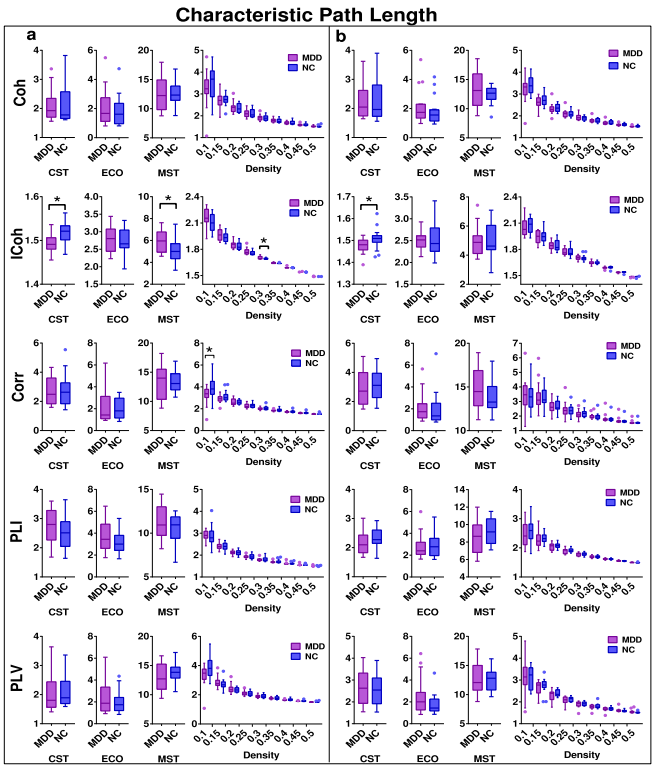

Fig. 1. **Characteristic Path Length (CPL) of EEG-based functional networks in MDD and NC in (a) theta band (4 - 8Hz) and (b) alpha band (8 - 13Hz).** The central lines in the boxplots indicate the median, purple and blue circles represent outliers of the MDD and NC respectively. And the asterisk indicates a significant difference ($p < 0.05$, non-parametric permutation test). Coupling methods included: coherence (Coh), imaginary part of coherence (ICoh), Pearson correlation coefficient (Corr), phase lag index (PLI) and phase lock value (PLV). Binarization approaches included: Cluster-Span Threshold (CST), Efficiency Cost Optimization threshold (ECO), Minimum Spanning Threshold (MST), and Density.

functional connectivity matrices were calculated every 4 s with a 2 s overlapping window for theta and alpha frequency bands [8]. In the end, we averaged functional connection matrices across all epochs to obtain the measures for each subject and each frequency band. Furthermore, in the following work, we would also study the differences between MDD and NC groups based on hubs and the symmetry of brain regions within groups based on degree, so we averaged connection matrices across subjects to obtain connection matrix for each group and each frequency band, which we called grouped functional connectivity matrix. The dimension of functional connectivity matrix was 128×128. Finally, individual and grouped functional connectivity matrices were converted into binary matrices according to the following binarization methods.

D. Binarization of Brain Networks

Due to weak and spurious connections were usually contained in functional networks, these links may obscure the topology of significant connections. So as to solve this problem binarization method may be a good candidate to remove the weak connections. In this study, we used CST, ECO, MST and Density to obtain binary brain networks (a detailed description of these binarization methods are in the supplementary material-B). Subsequently, all the binary brain network matrices obtained from coupling methods and binarization approaches were quantitatively analyzed using graph theory analysis.

E. Network Metrics

Graphs can be characterized by different measures [24]. In our study, we calculated integration and segregation network metrics for individual binary brain networks. The network metrics of functional integration included: 1) CPL, 2) Edge betweenness centrality (EBC), and 3) Node betweenness centrality (NBC). The network metrics of functional segregation included: 1) CC, and 2) Modularity (mathematical formula of the network metrics are in the supplementary material-C).

Subsequently, for the network metrics with significant differences between MDD and NC groups, we would examine the differences of these metrics among brain regions between two groups, for each subject we averaged the network metric for eight main brain regions, including left frontal region (LF), right frontal region (RF), left temporal region (LT), right temporal region (RF), left central region (LC), right central region (RC), left parietal-occipital region (LPO) and right parietal-occipital region (RPO). The partition rule is according to their anatomical position (detailed electrode sites of eight brain regions are in the supplementary material-D). This lobe-based EEG regional analysis is supported by previous studies [44], [45].

Moreover, we calculated hubs and degree for grouped binary brain networks. In the brain networks, hubs play an important role in efficient information communication and resilience [46]. A node can be considered as a hub if the degree of the node is at least one standard deviation above the mean degree of network [47]. Degree of a node is defined as the number of links connected to this node. Network metrics were calculated by Brain Connectivity Toolbox (http://www.brain-connectivity-toolbox.net/) used in Matlab R2017a.

III. Statistical Analysis and Classification

A. Differences in Network Metrics

In order to assess whether MDD and NC groups have statistically significant network metrics, a non-parametric permutation test [14] method was used. First, a t-value was calculated for each studied network metric (CPL, EBC, NBC, CC, Modularity and degree) as an observed test statistic between two groups. Next, each subject was randomly reallocated to either MDD or NC group, resulting in the same number of subjects for each group, so after permutation the number ratio of MDD and NC was still 16:16. The t-values were recalculated for the permutated groups 50000 times, and the null distribution of test statistics was obtained for the group difference. Finally, the proportion of sampled permutations where the t-values were greater than the observed test statistic was determined as the p-value of the observed group difference. A level of significance was $p < 0.05$. In addition, for the network metrics with significant differences between MDD and NC

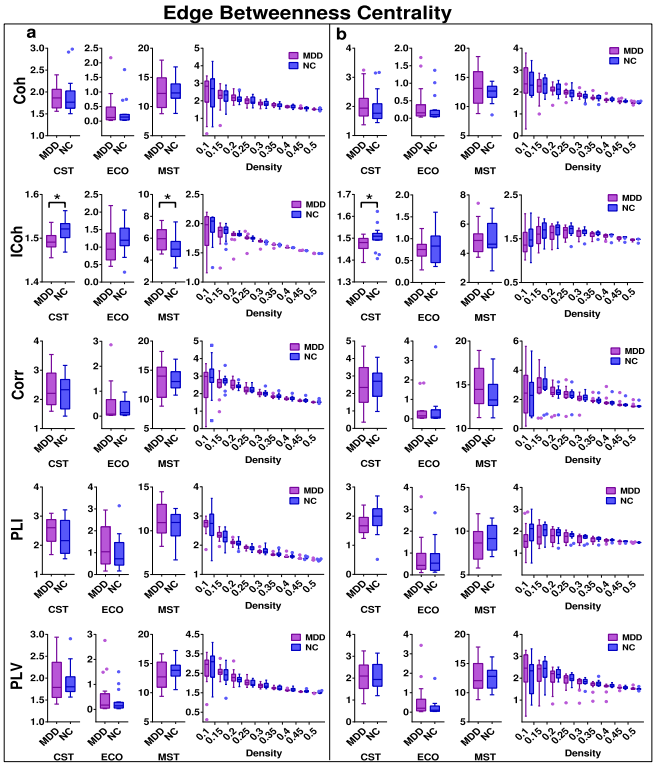

Fig. 2. **Edge Betweenness Centrality (EBC) of EEG-based functional networks in MDD and NC in (a) theta band (4 - 8Hz) and (b) alpha band (8 - 13Hz).** Other descriptions are as Fig 1.

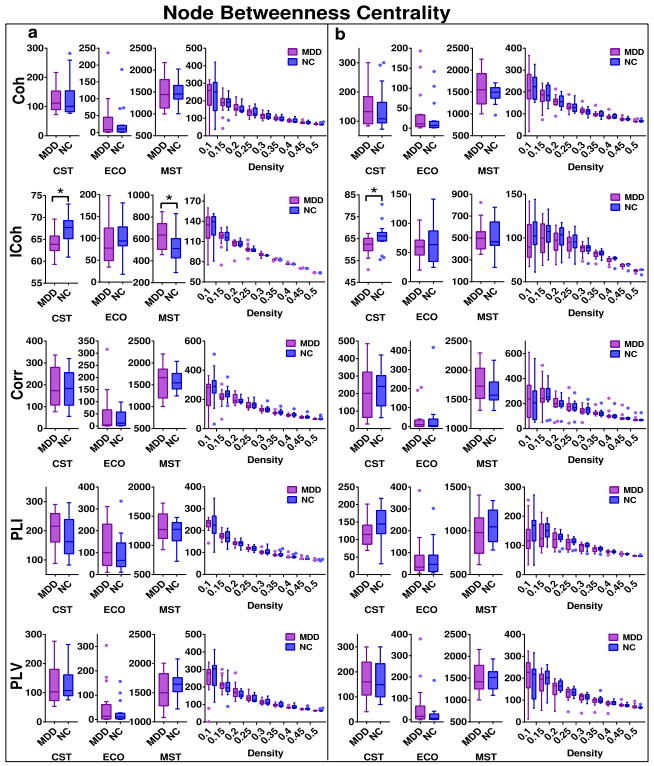

Fig. 3. **Node Betweenness Centrality (NBC) of EEG-based functional networks in MDD and NC in (a) theta band (4 - 8Hz) and (b) alpha band (8 - 13Hz).** Other descriptions are as Fig 1.

group, one-way ANOVA analysis was used to evaluate the statistical differences of these network metrics among eight brain regions between two groups, significance level p was set to 0.05. Analysis was performed using Matlab R2017a and SPSS (version 19).

B. Correlation Between Network Metrics and Clinic State

When any network metric between two groups had significant differences, we would assess the correlation between these network metrics and PHQ-9 score by Spearman correlation. A significance level of $p < 0.05$ was used. Furthermore, receiver operating characteristic (ROC) curve [48] and related area under the ROC curve (AUC) [49] were used to evaluate the ability of these network metrics to discriminate MDD from NC.

C. Classification Performance Evaluation of Network Metrics

To check whether network metrics having significant correlation with the PHQ-9 scores and having high AUC value could be able to classify MDD from NC, we chose Support Vector Machine (SVM) with RBF kernel based on previous studies [50], [51]. The classifier was executed for each network metric and for each frequency band with leave-one-out cross validation (LOOCV). The performance of the classifier was quantified using the accuracy, sensitivity and specificity based on the results of cross-validation. Note that accuracy represents the overall proportion of samples correctly predicted, sensitivity represents the proportion of patients with MDD correctly predicted, and specificity represents the proportion of normal controls correctly predicted. In addition, permutation test with 10000 times was also used to assess the classifier performance [3], the accuracy was the statistic.

IV. Results

A. Combination of Coupling Methods and Binarization Approaches

We used network metrics (CPL, EBC, NBC, CC and Modularity) of functional integration and segregation to assess the performance of coupling methods and binarization approaches. As shown in Fig 1a to 5a, for theta frequency band, when the connectivity values were estimated by ICoh, MDD networks showed significant decrease in the CPL when CST was used for binarization, but MDD networks showed significant increase in the CPL when MST and Density (30%) were used for binarization. And when the connectivity values were estimated by Corr, MDD networks also showed significant decrease in the CPL when Density (10%) was used (see Fig 1a). Similar pattern of EBC and NBC were also observed between MDD and NC, when the connectivity values were estimated by ICoh, MDD networks showed significant decrease in the EBC and NBC when CST was used for binarization, but contrary results were found in the EBC and NBC

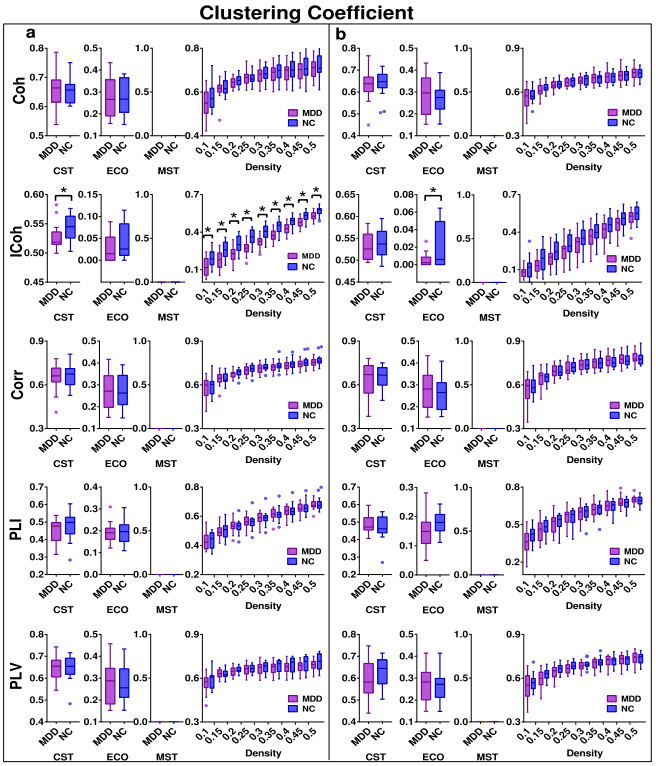

Fig. 4. **Clustering Coefficient (CC) of EEG-based functional networks in MDD and NC in (a) theta band (4 - 8Hz) and (b) alpha band (8 - 13Hz).** Other descriptions are as Fig 1.

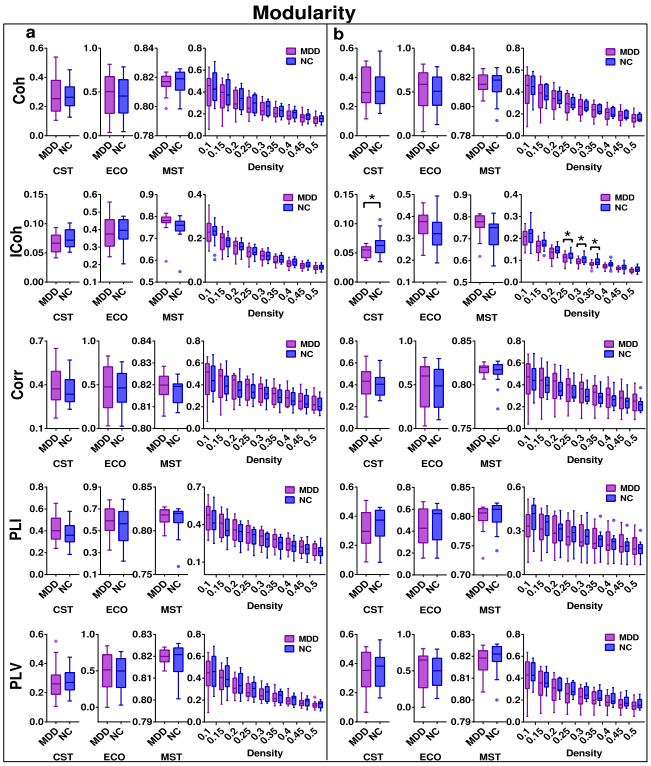

Fig. 5. **Modularity of EEG-based functional networks in MDD and NC in (a) theta band (4 - 8Hz) and (b) alpha band (8 - 13Hz).** Other descriptions are as Fig 1.

when MST were used for binarization (see Fig 2a and 3a). MDD exhibited reduced CC when coupling method ICoh and binarization approaches CST and Density (10%-50%) were used (see Fig 4a).

As shown in Fig 1b to 5b, for alpha frequency band, when the connectivity values were estimated by ICoh, MDD networks showed significant reduction in CPL, EBC, NBC, and Modularity when CST was used for binarization (see Fig 1b to 3b and 5b), otherwise, MDD also exhibited significant reduction in Modularity when Density (25%-35%) was used to binarize (see Fig 5b). MDD showed reduced CC when coupling method ICoh and binarization approach ECO were used (see Fig 4b). What should be noted was that CC calculated from network constructed by MST was zero, due to MST was a no-looping graph. And we found that network metrics had no significant differences between two groups in theta and alpha bands when other coupling methods (Coh, Corr, PLI and PLV) were used. So the combination of ICoh and CST outperformed other combined methods.

In this paper, all the functional brain networks were calculated every 4 s with a 2 s overlapping window for theta and alpha frequency bands. However, previous studies selected variable epoch length (from 1 to 16 s in step of 2 s) with non-overlapping windows, and they found MST parameters stabilized for epochs between 1 and 6 s based on PLI [52]. So we also tried to calculate the functional brain networks based on 4 s epoch length with non-overlapping windows (detailed results were provided in the supplementary material-E), which

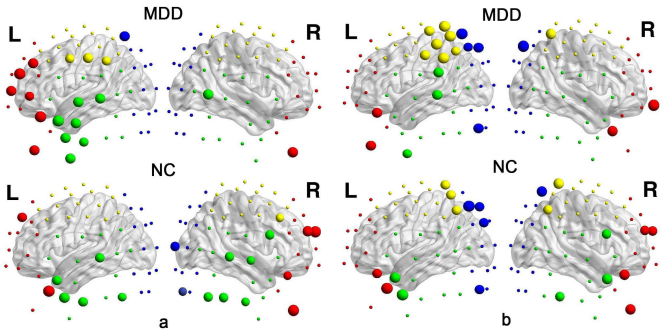

Fig. 6. **Distribution of hubs of MDD group and NC group in (a) theta band and (b) alpha band.** Nodes that are labeled represent network hubs. The volume of the spheres represents the degree of the corresponding brain region. Red color hubs represent frontal brain region, yellow color hubs represent central brain region, green color hubs represent temporal brain region, and blue color hubs represent parietal-occipital brain region.

also confirmed that the combination of ICoh and CST was optimal for MDD identification. Hence, we would further explore the aberrant network topology of MDD based on this combination method.

B. MDD-Related Alterations in Hubs Characteristic

The distribution of hubs in MDD and NC groups was shown in Fig 6. For theta frequency band (see Fig 6a), the hubs in the MDD group were mainly distributed in the left frontal, left temporal and left central brain regions. However, the

TABLE II
THE SYMMETRY RESULTS OF DEGREE AMONG BRAIN REGIONS WITHIN MDD GROUP AND NC GROUP IN THETA AND ALPHA BANDS

Frequency band	Group	LF *mean*± SD	RF *mean*± SD	p value	LT *mean*± SD	RT *mean*± SD	p value	LC *mean*± SD	RC *mean*± SD	p value	LPO *mean*± SD	RPO *mean*± SD	p value
theta	MDD	**76.54 ± 17.31**	**59.62 ± 15.26**	**0.016**	70.00±23.11	60.29±11.95	0.136	55.44±22.60	51.38±16.17	0.568	50.62±17.05	50.15±16.77	0.954
	NC	63.69±20.62	66.54±28.33	0.777	58.71±22.81	65.12±20.08	0.396	45.31±20.65	42.94±17.93	0.734	50.62±14.85	54.00±18.38	0.617
alpha	MDD	62.00±15.94	64.46±17.05	0.714	**57.53 ± 24.74**	**38.65 ± 22.77**	**0.028**	**73.69 ± 21.43**	**49.25 ± 17.88**	**0.002**	63.38±23.45	53.62±19.23	0.259
	NC	58.92±22.95	68.69±20.91	0.271	52.59±27.22	60.65±20.02	0.337	59.50±20.53	52.88±22.94	0.393	64.00±25.65	56.77±20.38	0.435

Note: LF represents Left Frontal brain region, RF represents Right Frontal brain region, LT represents Left Temporal brain region, RT represents Right Temporal brain region, LC represents Left Central brain region, RC represents Right Central brain region, LPO represents Left Parietal-Occipital brain region, RPO represents Right Parietal-Occipital brain region. Bold represents having significant statistics difference ($p < 0.05$, non-parametric permutation test with 50000 times).

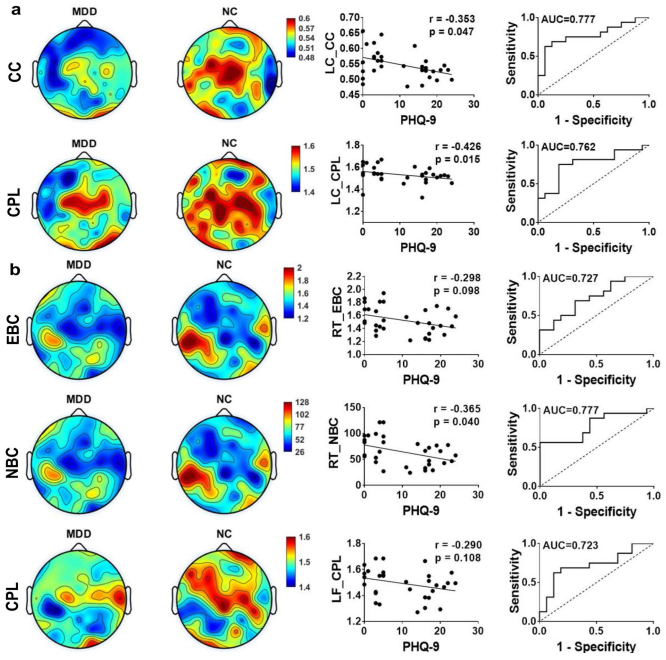

Fig. 7. **The topography and ROC curves of significant network metrics between MDD group and NC group and the relationship between these network properties with PHQ-9 scores in (a) theta and (b) alpha frequency bands.** r is the correlation coefficient, p is the statistic value. The ROC curve is plotted using a solid line. AUC represent area under the ROC curve.

hubs in the NC group were mainly distributed in frontal and temporal brain regions. For alpha frequency band (see Fig 6b), the network hubs identified in MDD group were in frontal, left temporal, left central and left parietal-occipital brain areas, whereas network hubs in NC group were in frontal, temporal, central and parietal-occipital brain areas. According to the above results, we found that hubs in MDD mainly distributed in left hemisphere, but hubs in NC were distributed in both of left and right hemispheres. We speculated that asymmetry may exist in MDD group. So we studied symmetry among brain regions within MDD group and NC group based on degree (see below).

C. MDD-Related Symmetry in Brain Regions

The symmetry results of degree among brain regions within MDD group and NC group in theta and alpha band was shown in Table 2. From Table 2 we found that asymmetry of brain regions did exist in MDD group, but not in the NC group. For theta frequency band, the degree in LF (76.54 ± 17.31) of MDD was remarkably higher than that of RF (59.62 ± 15.26, $p = 0.016$). For alpha frequency band, the degree in LT (57.53 ± 24.74) of MDD was remarkably higher than that of RT (38.65 ± 22.77, $p = 0.028$). And the degree in LC (73.69 ± 21.43) of MDD was also significantly higher than that of RC (49.25 ± 17.88, $p = 0.002$).

D. MDD-Related Biomarkers in Network Metrics

According to Fig 1 to 5, we concluded that CC, EBC, NBC and CPL in theta band and Modularity, EBC, NBC and CPL in alpha band had significant differences between MDD group and NC group. So we further examined the differences of the mean values of these metrics for eight brain regions between two groups in theta and alpha bands, results were shown in Table 3. For theta frequency band, MDD had significant lower CC values ($p < 0.05$) at LF and LC and lower CPL value ($p < 0.05$) at LC, whereas no significant differences were found at other brain regions. Neither EBC value nor NBC value showed difference between two groups. For alpha frequency band, MDD showed significantly lower both of EBC values ($p < 0.05$) and NBC values ($p < 0.05$) at RT, and also had decreased CPL values ($p < 0.05$) at LF, whereas no significant differences were found at other brain regions. Modularity value showed no differences between two groups.

For the purpose to find out potential biomarkers that can effectively detect depression. We assessed the relationships between the network metrics having significant differences and the PHQ-9 score, performing Spearman correlation analysis. And we also evaluated the ability of these network metrics to discriminate MDD patients from NC, using ROC plots. Results were in Fig 7. For theta band, the CC in the LC and LF was negatively correlated with PHQ-9 scores ($p < 0.05$), and the AUC value were 0.777 and 0.664 respectively (note: AUC value less than 0.70 indicates the precision of the diagnostic test is poor, so the ROC curve of CC in the LF is not shown in Fig 7.), and the CPL in the LC showed significant negatively correlation with PHQ-9 scores ($p < 0.05$), the AUC value was 0.762. The brain topology of CC and CPL indicated depression group was lower than normal group, especially in central (see Fig 7a). For alpha band, the NBC in the RT was negatively

TABLE III
ONE-WAY ANOVA RESULTS OF THE AVERAGE VALUES OF SIGNIFICANT NETWORK METRICS FOR EIGHT BRAIN REGIONS BETWEEN MDD AND NC GROUPS IN THETA AND ALPHA BANDS

Brain region		LF		RF		LT		RT		LC		RC		LPO		RPO	
Frequency band	Network features	MDD	NC	MDD	NC	MDD	NC	MDD	NC	MDD	NC	MDD	NC	MDD	NC	MDD	NC
theta	CC	**0.514**	**0.540**	0.514	0.535	0.518	0.547	0.533	0.523	**0.527**	**0.568**	0.535	0.557	0.538	0.545	0.534	0.541
	EBC	1.550	1.580	1.507	1.614	1.591	1.513	1.506	1.621	1.460	1.400	1.425	1.424	1.470	1.475	1.433	1.518
	NBC	71.350	75.181	65.841	79.553	76.687	66.670	65.824	80.424	59.895	52.160	55.418	55.273	61.191	61.745	56.375	67.259
	CPL	1.469	1.497	1.488	1.483	1.465	1.515	1.481	1.486	**1.505**	**1.558**	1.514	1.548	1.500	1.525	1.516	1.525
alpha	Modularity	1.606	1.486	1.673	1.616	1.632	1.787	1.610	1.610	1.539	1.617	1.652	1.520	1.702	1.673	1.553	1.668
	EBC	1.523	1.395	1.504	1.456	1.481	1.550	**1.443**	**1.608**	1.460	1.521	1.443	1.441	1.452	1.548	1.489	1.491
	NBC	68.730	51.663	66.279	59.522	63.244	72.461	**57.879**	**78.955**	60.111	67.862	57.907	57.622	59.038	71.282	63.731	63.984
	CPL	**1.454**	**1.533**	1.445	1.516	1.478	1.485	1.498	1.485	1.470	1.508	1.486	1.526	1.475	1.493	1.481	1.517

Note: Bold represents having significant statistics difference ($p < 0.05$, One-way ANOVA analysis). CC represents Clustering Coefficient, EBC represents Edge Betweenness Centrality, NBC represents Node Betweenness Centrality, CPL represents Characteristic Path Length.

TABLE IV
CLASSIFICATION PERFORMANCE EVALUATION OF NETWORK METRICS (LC-CC, LC-CPL, RT-NBC)

Frequency band	network metrics	Accuracy	Sensitivity	Specificity	p value
theta	LC-CC	78.13%	87.50%	68.75%	0.0006
	LC-CPL	65.63%	68.75%	62.50%	0.0553
alpha	RT-NBC	87.50%	93.75%	81.25%	0.0001

Note: Classifier is SVM with RBF kernel and is executed with LOOCV. LC-CC is Clustering Coefficient of Left Central brain region, LC-CPL is Characteristic Path Length of Left Central brain region, RT-NBC is Node betweenness Centrality of Right Temporal brain region. P value is obtained by permutation test.

($p < 0.05$) correlated with PHQ-9 scores, the AUC value was 0.777, and the EBC in the RT showed marginally significant ($0.05 < p < 0.1$) correlation with PHQ-9 scores, the AUC value were 0.727. However, the CPL in the LF showed no correlation with PHQ-9 ($p > 0.05$), the AUC value was 0.723. The brain topology of EBC, NBC and CPL indicated depression group was lower than normal group, especially temporal of EBC and NBC and frontal of CPL (see Fig 7b).

However, in order to better prove whether these network metrics were able to classify MDD from NC, Network metrics (CC and CPL of LC in the theta band, and NBC of RT in the alpha band) having significant correlation with the PHQ-9 scores and having high AUC value were further used as feature vectors. Classification results were shown in the Table 4. For theta frequency band, when CC in the LC was used as feature vector, classification accuracy achieved 78.13% ($p < 0.05$), sensitivity achieved 87.50% and specificity achieved 68.75%; when CPL in the LC was used as feature vector, classification accuracy was 65.63% ($p > 0.05$), sensitivity was 68.75% and specificity was 62.50%. For alpha frequency band, classification accuracy yielded 87.50% ($p < 0.05$), sensitivity yielded 93.75% and specificity yielded 81.25%, when NBC in the RT was used as feature. So the network metrics: CC of LC in the theta band and NBC of RT in the alpha band had the ability to discriminate MDD from NC.

V. DISCUSSION

This study used functional connectivity and graph theory analysis to investigate the topological alterations of high-density resting state EEG functional brain networks in patients with MDD. Our main findings were: (1) ICoh was used to estimate the connectivity matrix and CST was used for binarization which could achieve effective MDD identification; (2) the hubs in MDD was predominant in left hemisphere; (3) symmetry breaking existed in MDD, especially frontal in theta band, and temporal and central in alpha band; (4) decreased CC, CPL, EBC, NBC and Modularity in MDD revealed that patients with MDD had more random network structure, altered CC in the LC in theta band and altered NBC in the RT in alpha band were negative correlated with PHQ-9 score, and had good discrimination ability for depression. In conclusion, our findings confirmed that the functional topological structure of resting state brain network is disrupted in MDD, and provide reliable methods and sensitive biomarkers that can be used for probable MDD diagnosis.

A. Why the Combination of ICoh and CST Is Optimal?

In this pilot study, we try to adopt different coupling methods to construct functional connectivity matrices and binarization approaches to binarize functional networks, which not only including some methods (coupling methods: ICoh, PLV, binarization approach: CST, ECO) that haven't been used in MDD, but also including some methods (coupling methods: Coh, Corr, PLI, binarization approach: MST, Density) that have been applied to MDD. However, in this research, topological metrics of networks constructed using ICoh method and CST binarization show more significant difference between MDD patients and NC than the other methods. However network metrics computed by other methods do not have distinct differences between two groups, the reasons we analyzed may be influenced by the reference electrode. Previous research has observed the network properties computed from functional brain networks are significantly affected by the EEG reference choice [32]. Our study used REST, other researches used AVE, DLM and Cz. So using different reference schemes may come to different conclusions. But REST has been proved significantly decreased the distortion of connectivity patterns than other reference techniques [32], [53]. Hence, the study of functional connectivity patterns using high-density EEG system [21] based-on REST reference can obtain more reliable results.

In addition, commonly used coupling methods (Coh, Corr, PLV) face limitations caused by volume conduction when dealing with sensor layer EEG data [54]. ICoh and PLI are robust to artefacts of volume conduction [19], [20]. But in this paper when using PLI to construct functional connectivity matrices, network properties of functional brain network did not show significant differences between MDD and NC groups, which may be affected by the epoch length [52]. And a research has demonstrated that the performance of other functional connectivity methods was strongly influenced by the number of sample available for the estimation process [55], which maybe also exist in the ICoh. So in the future work, we will explore how the epoch length affect ICoh. As we know ICoh method has been proved useful for functional connectivity analysis when applying to various datasets [56], [57]. So ICoh may be a good choice for functional connectivity of MDD. For binarization approach Density is arbitrary and subjective. Though MST and ECO are unbiased and non-arbitrary, these two methods leads to highly sparse networks (MST and ECO networks with N nodes respectively has N-1 edges and 1.5N edges), thus some important connections information maybe absent, in turn resulting in insensitive to more subtle differences in cognitive function [28]. And MST and ECO are still sensitive to network size [8]. Moreover, a recent study indicates that when there are differences in overall functional connectivity between two groups, we should carefully choose Density binarization approach, because even a small difference in functional connectivity can have a potential impact on the between-groups differences of network metrics (e.g. global efficient and CC) [58]. What should we note is that MST or ECO approach can be seen as one of the strictest cases of Density, hence MST or ECO may also face the same problems of Density. When using Density, MST and ECO to binarize the functional networks, the network metrics computed from these binary brain networks almost have not significant differences between MDD group and NC group, which may due to in this paper there is no evident differences of functional connectivity between two groups. However, CST is from a novel perspective to select the threshold, which chooses the threshold by adjusting the ratio of closed to open triples to reach balance, rather than fixing connection density at an arbitrary value. This method can ensure a trade-off of sparsity and density of information [28]. CST captures the differences found at both high and low threshold levels, which may make different network metrics become more sensitive [28]. There are researches indicated that CST outperforms the MST, ECO and Density [21], [59]. Therefore, according to the above analysis, we conclude that the combination of coupling method ICoh and binarization approach CST is optimal to explore the aberrant brain network topology structure of MDD.

B. Aberrant Brain Network Structure and Potential Biomarkers in MDD

In this paper, we continued to study the alteration of brain network architecture of MDD based on ICoh coupling method and CST binarization approach. Our results revealed that the topology distribution of hubs of patients with MDD had an aberrant patterns compared to NC. Specifically, the hubs of MDD mainly distributed in left frontal, left temporal and left central regions in theta band, and in frontal, left temporal, left central and left parietal-occipital regions in alpha band. But hubs in NC group distributed both in left and right hemispheres. Aiming at the phenomenon of hubs of MDD mainly distributed in left hemisphere, we speculate that patients with MDD have abnormal information processing, which is consistent with the right hemisphere dysfunction in depression [60]. Early behavioral studies indicated that right hemisphere of depressed patients showed greater deficits in functions compared to left hemisphere [61]. A previous EEG study reported in-degree of left hemisphere in depressed patients was larger than that of right hemisphere, which indicated that left hemisphere was strongly influenced by its right hemisphere in depressed patients [34]. Left hemisphere lateralization found in this study might be a characteristic of cognition functional impairment in MDD, which needs more researches to further study the information processing mechanisms of MDD.

Asymmetry has great contribution to revealing the intrinsic properties of MDD. Many EEG studies have found asymmetric connection patterns within the frontal region of patients with MDD compared to NC in theta and alpha bands [42], [62]. And frontal lobe is proven to be an important part related to MDD [63]. Similar results were found in our study, symmetry breaking was found in frontal lobe (degree of LF > degree of RF) in theta band for MDD. But we also obtained different results that for alpha band asymmetry was found in temporal lobe (degree of LT > degree of RT) and central lobe (degree of LC > degree of RC) of MDD. Previous studies also concluded the alpha asymmetry at parietal region in depressed patients, which showed less activity over right parietal than left parietal, when compared to healthy individuals [64]. Likewise, there was a study found that right temporal region dysfunction may be particularly evident in melancholic depression [65], which can further support our findings.

In addition, our results also revealed the brain networks structure of MDD patients tended to be randomized. MDD exhibited decreased CC, EBC, NBC and CPL in theta band and Modularity, EBC, NBC and CPL in alpha band, when compared to NC group, which are consistent with the results of previous studies [12], [14], [27], [66]. Specifically, we found CC and CPL of LC in theta band and NBC of RT in alpha band were significantly negatively related to the PHQ-9 scores, indicating the more severe the depression, the lower the CC and NBC. These correlations have been found in previous studies. For example, a comparable study found that the CC of the left amygdala was negatively related to the scores of Hamilton Depression Rating Scale-17 (HAMD-17), PHQ-9 and Trait Anxiety Inventory (T-AI) [14]. Another study suggested that reduced CC of the prefrontal cortex, striatum, and medial temporal cortex are likely to be associated with the generation of depressive symptoms, such as persistent sadness, guilt, worthlessness, and recurrent reflective self-focus [67]. From the view of node centrality, Zhang *et al.* [68] found the node centrality of the left hippocampus and the left caudate nucleus were significantly related to the course and severity of depression. Furthermore, related studies suggested

that temporal lobe also plays a vital role in depression studies. For example, Fan *et al.* [69] claimed that aberrant right superior temporal gyrus activity might be a potential marker of suicide tendency in MDD. And Blackhart *et al.* [70] suggested relatively less right parietotemporal activity was correlated with higher depression scores. These findings confirmed the validity of results obtained from this study. More importantly, when network metrics CC of LC in the theta band and NBC of RT in the alpha band were used as feature vectors respectively, the classification accuracy achieved above 78.00%. Especially, when network metric NBC of RT in the alpha band was used as feature, classification accuracy was 87.50%, sensitivity was 93.70% and specificity was 81.25%. Our results are equal or better than previous research [11], [12], [71]. So the network metrics computed in our study have the ability to discriminate patients with MDD from NC.

VI. Conclusion

To explore reliable and robust construction methods of functional brain networks, this study systematically compared the combination of different coupling methods (Coh, ICoh, Corr, PLI, PLV) and binarization approaches (CST, ECO, MST, Density) using high-density 128-channel resting state EEG recordings of MDD patients. We found that the combination of ICoh and CST was optimal. Applying this combination to further explore the aberrant brain network structure in MDD, we found right hemisphere function deficiency existed in MDD. Symmetry breaking was found in frontal lobe in theta band and in temporal lobe and central lobe in alpha band for MDD. Randomized brain topology structure likewise was found in MDD. These results confirmed that patients with MDD had abnormal information processing. Moreover, clustering coefficient in left central region in theta band and node betweenness centrality in right temporal region in alpha band were significantly negatively correlated with depressive level. And these network metrics possessed the ability to discriminate patients with MDD from NC, which may offer effective electrophysiological characteristics for probable MDD diagnosis. In summary, these findings provided insights into our understanding of aberrant topology organization in functional brain networks of MDD.

References

[1] Z. Jia *et al.*, "High-field magnetic resonance imaging of suicidality in patients with major depressive disorder," *Amer. J. Psychiatry*, vol. 167, no. 11, pp. 1381–1390, 2010.

[2] M. D. Greicius *et al.*, "Resting-state functional connectivity in major depression: Abnormally increased contributions from subgenual cingulate cortex and thalamus," *Biol. Psychiatry*, vol. 62, no. 5, pp. 429–437, 2007.

[3] L.-L. Zeng *et al.*, "Identifying major depression using whole-brain functional connectivity: A multivariate pattern analysis," *Brain A, J. Neurol.*, vol. 135, no. 5, pp. 1498–1507, 2012.

[4] A. Dutta, S. Mckie, and J. F. W. Deakin, "Resting state networks in major depressive disorder," *Psychiatry Res.*, vol. 224, no. 3, pp. 139–151, 2014.

[5] K. RH *et al.*, "Large-scale network dysfunction in major depressive disorder: A meta-analysis of resting-state functional connectivity," *Jama Psychiatry*, vol. 72, no. 6, p. 603, 2015.

[6] V. Sakkalis, "Review of advanced techniques for the estimation of brain connectivity measured with EEG/MEG," *Comput. Biol. Med.*, vol. 41, no. 12, pp. 1110–1117, 2011.

[7] A. A. Fingelkurts, A. A. Fingelkurts, and S. Kähkönen, "Functional connectivity in the brain—Is it an elusive concept?" *Neurosci. Biobehav. Rev.*, vol. 28, no. 8, pp. 827–836, 2005.

[8] D. E. Van *et al.*, "Opportunities and methodological challenges in EEG and meg resting state functional brain network research," *Clin. Neurophysiol.*, vol. 126, no. 8, pp. 1468–1481, 2014.

[9] A. Griffa *et al.*, "Transient networks of spatio-temporal connectivity map communication pathways in brain functional systems," *NeuroImage*, vol. 155, pp. 490–502, Jul. 2017.

[10] H. Yu *et al.*, "Synchrony dynamics underlying effective connectivity reconstruction of neuronal circuits," *Phys. A, Stat. Mech. Appl.*, vol. 471, pp. 674–687, Apr. 2017.

[11] A. F. Leuchter, I. A. Cook, A. M. Hunter, C. Cai, and S. Horvath, "Resting-state quantitative electroencephalography reveals increased neurophysiologic connectivity in depression," *PLoS ONE*, vol. 7, no. 2, p. e32508, 2012.

[12] L. Orgo, M. Bachmann, K. Kalev, M. Järvelaid, J. Raik, and H. Hinrikus, "Resting EEG functional connectivity and graph theoretical measures for discrimination of depression," in *Proc. IEEE Embs Int. Conf. Biomed. Health Inform.*, Feb. 2017, pp. 389–392.

[13] X. Li *et al.*, "A resting-state brain functional network study in MDD based on minimum spanning tree analysis and the hierarchical clustering," *Complexity*, vol. 2017, no. 1, 2017, Art. no. 9514369.

[14] M. Zhang *et al.*, "Randomized EEG functional brain networks in major depressive disorders with greater resilience and lower rich-club coefficient," *Clin. Neurophysiol.*, vol. 129, no. 4, pp. 743–758, 2018.

[15] D. L. García *et al.*, "The imaginary part of coherency in autism: Differences in cortical functional connectivity in preschool children," *PLoS ONE*, vol. 8, no. 10, p. e75941, 2013.

[16] J.-M. Schoffelen and J. Gross, "Source connectivity analysis with MEG and EEG," *Hum. Brain Mapping*, vol. 30, no. 6, pp. 1857–1865, 2009.

[17] L. Cai, X. Wei, J. Wang, H. Yu, B. Deng, and R. Wang, "Reconstruction of functional brain network in Alzheimer's disease via cross-frequency phase synchronization," *Neurocomputing*, vol. 314, pp. 490–500, Nov. 2018.

[18] H. Yu, X. Wu, L. Cai, B. Deng, and J. Wang, "Modulation of spectral power and functional connectivity in human brain by acupuncture stimulation," *IEEE Trans. Neural Syst. Rehabil. Eng.*, vol. 26, no. 5, pp. 977–986, May 2018.

[19] G. Nolte, O. Bai, L. Wheaton, Z. Mari, S. Vorbach, and M. Hallett, "Identifying true brain interaction from EEG data using the imaginary part of coherency," *Clin. Neurophysiol.*, vol. 115, no. 10, pp. 2292–2307, 2004.

[20] C. J. Stam, G. Nolte, and A. Daffertshofer, "Phase lag index: Assessment of functional connectivity from multi channel EEG and MEG with diminished bias from common sources," *Hum. Brain Mapping*, vol. 28, no. 11, pp. 1178–1193, 2007.

[21] K. Smith, D. Abásolo, and J. Escudero, "Accounting for the complex hierarchical topology of EEG phase-based functional connectivity in network binarisation," *PLoS ONE*, vol. 12, no. 10, p. e0186164, 2017.

[22] J. Wang, X. Zuo, and Y. He, "Graph-based network analysis of resting-state functional MRI," *Frontiers Syst. Neurosci.*, vol. 4, no. 16, p. 16, 2010.

[23] Y. He and A. Evans, "Graph theoretical modeling of brain connectivity," *Current Opinion Neurol.*, vol. 23, no. 4, pp. 341–350, 2010.

[24] M. Rubinov and O. Sporns, "Complex network measures of brain connectivity: Uses and interpretations," *NeuroImage*, vol. 52, no. 3, pp. 1059–1069, 2010.

[25] C. Meng *et al.*, "Aberrant topology of striatum's connectivity is associated with the number of episodes in depression," *Brain A J. Neurol.*, vol. 137, no. 2, p. 598, 2014.

[26] M. S. Korgaonkar *et al.*, "Abnormal structural networks characterize major depressive disorder: A connectome analysis," *Biol Psychiatry*, vol. 76, no. 7, pp. 567–574, 2014.

[27] Y. Li, D. Cao, L. Wei, Y. Tang, and J. Wang, "Abnormal functional connectivity of EEG gamma band in patients with depression during emotional face processing," *Clin. Neurophysiol.*, vol. 126, no. 11, pp. 2078–2089, 2015.

[28] K. Smith, H. Azami, M. A. Parra, J. M. Starr, and J. Escudero, "Cluster-span threshold: An unbiased threshold for binarising weighted complete networks in functional connectivity analysis," in *Proc. IEEE Conf. Eng. Med. Biol. Soc.*, Aug. 2015, pp. 2840–2843.

[29] V. F. F. De, V. Latora, and M. Chavez, "A topological criterion for filtering information in complex brain networks," *PLoS Comput. Biol.*, vol. 13, no. 1, p. e1005305, 2017.

[30] J. B. Kruskal, Jr., "On the shortest spanning subtree of a graph and the traveling salesman problem," *Proc. Amer. Math. Soc.*, vol. 7, no. 1, pp. 48–50, Feb. 1956.

[31] R. Kalpana and I. Gnanambal, "The analysis of nonlinear invariants of multi-channel EEG signal using graph-theory connectivity approach in patient with depression," *Asian J. Inf. Technol.*, vol. 15, no. 20, pp. 4106–4112, 2016.

[32] F. Chella, V. Pizzella, F. Zappasodi, and L. Marzetti, "Impact of the reference choice on scalp EEG connectivity estimation," *J. Neural Eng.*, vol. 13, no. 3, p. 036016, 2016.

[33] M. D. Holmes, D. M. Tucker, J. M. Quiring, S. Hakimian, J. W. Miller, and J. G. Ojemann, "Comparing noninvasive dense array and intracranial electroencephalography for localization of seizures," *Neurosurgery*, vol. 66, no. 2, pp. 354–362, 2010.

[34] Y. Sun, S. Hu, J. Chambers, Y. Zhu, and S. Tong, "Graphic patterns of cortical functional connectivity of depressed patients on the basis of EEG measurements," in *Proc. Int. Conf. IEEE Eng. Med. Biol. Soc. (Embc)*, Aug./Sep. 2011, pp. 1419–1422.

[35] D. V. Sheehan *et al.*, "The mini-international neuropsychiatric interview (M.I.N.I): The development and validation of a structured diagnostic psychiatric interview for DSM-IV and ICD-10," *J. Clin. Psychiatry*, vol. 59, no. 20, pp. 22–33, 1998.

[36] L. L. T. N. Do, *American Psychiatric Association Diagnostic and Statistical Manual of Mental Disorders (DSM-IV)*. New York, NY, USA: Springer, 2011.

[37] R. L. Spitzer, K. Kroenke, and J. B. W. Williams, "Validation and utility of a self-report version of PRIME-MD: The PHQ primary care study," *JAMA*, vol. 282, no. 18, pp. 1737–1744, 1999.

[38] R. L. Spitzer *et al.*, "A brief measure for assessing generalized anxiety disorder: The GAD-7," *Arch. Internal Med.*, vol. 166, no. 10, pp. 1092–1097, 2006.

[39] T. C. Ferree, P. Luu, G. S. Russell, and D. M. Tucker, "Scalp electrode impedance, infection risk, and EEG data quality," *Clin. Neurophysiol.*, vol. 112, no. 3, pp. 536–544, 2001.

[40] D. Yao, "A method to standardize a reference of scalp EEG recordings to a point at infinity," *Physiol. Meas.*, vol. 22, no. 4, pp. 693–711, 2001.

[41] B. Hu *et al.*, "EEG-based cognitive interfaces for ubiquitous applications: Developments and challenges," *IEEE Intell. Syst.*, vol. 26, no. 5, pp. 46–53, Sep./Oct. 2011.

[42] A. A. Fingelkurts, A. A. Fingelkurts, H. Rytsälä, K. Suominen, E. Isometsä, and S. Kähkönen, "Impaired functional connectivity at EEG alpha and theta frequency bands in major depression," *Hum. Brain Mapping*, vol. 28, no. 3, pp. 247–261, 2007.

[43] G. E. Bruder, J. W. Stewart, and P. J. Mcgrath, "Right brain, left brain in depressive disorders: Clinical and theoretical implications of behavioral, electrophysiological and neuroimaging findings," *Neurosci. Biobehav. Rev.*, vol. 78, pp. 178–191, Jul. 2017.

[44] T. J. Whitford, C. J. Rennie, S. M. Grieve, C. R. Clark, E. Gordon, and L. M. Williams, "Brain maturation in adolescence: Concurrent changes in neuroanatomy and neurophysiology," *Hum. Brain Mapping*, vol. 28, no. 3, pp. 228–237, 2007.

[45] Z. Bian, Q. Li, L. Wang, C. Lu, S. Yin, and X. Li, "Relative power and coherence of EEG series are related to amnestic mild cognitive impairment in diabetes," *Frontiers Aging Neurosci.*, vol. 6, no. 3, p. 11, 2014.

[46] E. Bullmore and O. Sporns, "Complex brain networks: Graph theoretical analysis of structural and functional systems," *Nature Rev. Neurosci.*, vol. 10, no. 3, pp. 186–198, Mar. 2009.

[47] S. M. H. Hosseini, F. Hoeft, and S. R. Kesler, "GAT: A graph-theoretical analysis toolbox for analyzing between-group differences in large-scale structural and functional brain networks," *PLoS ONE*, vol. 7, no. 7, p. e40709, 2012.

[48] M. H. Zweig and G. Campbell, "Receiver-operating characteristic (ROC) plots: A fundamental evaluation tool in clinical medicine," *Clin. Chem.*, vol. 39, no. 4, pp. 561–577, 1993.

[49] J. Toppi *et al.*, "Measuring the agreement between brain connectivity networks," in *Proc. IEEE 38th Annu. Int. Conf. Eng. Med. Biol. Soc. (EMBC)*, Aug. 2016, pp. 68–71.

[50] J. Toppi, D. Mattia, M. Risetti, R. Formisano, F. Babiloni, and L. Astolfi, "Testing the significance of connectivity networks: Comparison of different assessing procedures," *IEEE Trans. Bio-Med. Eng.*, vol. 63, no. 12, pp. 2461–2473, Dec. 2016.

[51] H. Yu, X. Lei, Z. Song, J. Wang, X. Wei, and B. Yu, "Functional brain connectivity in Alzheimer's disease: An EEG study based on permutation disalignment index," *Phys. A, Stat. Mech. Appl.*, vol. 506, pp. 1093–1103, Sep. 2018.

[52] M. Fraschini, M. Demuru, A. Crobe, F. Marrosu, C. J. Stam, and A. Hillebrand, "The effect of epoch length on estimated EEG functional connectivity and brain network organisation," *J. Neural Eng.*, vol. 13, no. 3, p. 036015, 2016.

[53] P. Xu *et al.*, "Recognizing mild cognitive impairment based on network connectivity analysis of resting EEG with zero reference," *Physiol. Meas.*, vol. 35, no. 7, pp. 1279–1298, 2014.

[54] G. Alamian *et al.*, "Alterations of intrinsic brain connectivity patterns in depression and bipolar disorders: A critical assessment of magnetoencephalography-based evidence," *Frontiers Psychiatry*, vol. 8, no. 3, p. 41, 2017.

[55] Y. Antonacci, J. Toppi, S. Caschera, A. Anzolin, D. Mattia, and L. Astolfi, "Estimating brain connectivity when few data points are available: Perspectives and limitations," in *Proc. 39th Annu. Int. Conf. IEEE Eng. Med. Biol. Soc. (EMBC)*, Jul. 2017, pp. 4351–4354.

[56] J. M. S. Bornot, K. F. Wong-Lin, A. L. Ahmad, and G. Prasad, "Robust EEG/MEG based functional connectivity with the envelope of the imaginary coherence: Sensor space analysis," *Brain Topogr.*, vol. 31, no. 6, pp. 895–916, 2018.

[57] V. De Vico Fallani *et al.*, "Multiscale topological properties of functional brain networks during motor imagery after stroke," *NeuroImage*, vol. 83, no. 11, pp. 438–449, 2013.

[58] M. P. van den Heuvel, S. C. de Lange, A. Zalesky, C. Seguin, B. T. T. Yeo, and R. Schmidt, "Proportional thresholding in resting-state fmri functional connectivity networks and consequences for patient-control connectome studies: Issues and recommendations," *NeuroImage*, vol. 152, pp. 437–449, May 2017.

[59] K. Smith, D. Abasolo, and J. Escudero, "A comparison of the cluster-span threshold and the union of shortest paths as objective thresholds of EEG functional connectivity networks from Beta activity in Alzheimer's disease," in *Proc. Eng. Med. Biol. Soc.*, Aug. 2016, pp. 2826–2829.

[60] P. Florhenry, "Lateralized temporal-limbic dysfunction and psychopathology," *Ann. New York Acad. Sci. USA*, vol. 4, no. 5, pp. 578–590, 2003.

[61] R. Abrams, J. Redfield, and M. A. Taylor, "Cognitive dysfunction in schizophrenia, affective disorder and organic brain disease," *Brit. J. Psychiatry J. Mental Sci.*, vol. 139, no. 3, p. 190, 1981.

[62] D. Keeser *et al.*, "Changes of resting-state EEG and functional connectivity in the sensor and source space of patients with major depression," *Klinische Neurophysiologie*, vol. 44, no. 1, p. P142, 2013.

[63] T. Matsubara *et al.*, "Prefrontal activation in response to emotional words in patients with bipolar disorder and major depressive disorder," *NeuroImage*, vol. 85, no. 2, pp. 489–497, 2014.

[64] S. A. Reid, L. M. Duke, and J. J. B. Allen, "Resting frontal electroencephalographic asymmetry in depression: Inconsistencies suggest the need to identify mediating factors," *Psychophysiology*, vol. 35, no. 4, pp. 389–404, 1998.

[65] N. Tsujii *et al.*, "Right temporal activation differs between melancholia and nonmelancholic depression: A multichannel near-infrared spectroscopy study," *J. Psychiatric Res.*, vol. 55, no. 1, pp. 1–7, 2014.

[66] M. K. Singh *et al.*, "Anomalous gray matter structural networks in major depressive disorder," *Biol. Psychiatry*, vol. 74, no. 10, pp. 777–785, 2013.

[67] V. Menon, "Large-scale brain networks and psychopathology: A unifying triple network model," *Trends Cognit. Sci.*, vol. 15, no. 10, pp. 483–506, 2011.

[68] J. Zhang *et al.*, "Disrupted brain connectivity networks in drug-naive, first-episode major depressive disorder," *Biol. Psychiatry*, vol. 70, no. 4, pp. 334–342, 2011.

[69] T. Fan, X. Wu, L. Yao, and J. Dong, "Abnormal baseline brain activity in suicidal and non-suicidal patients with major depressive disorder," *Neurosci. Lett.*, vol. 534, no. 1, pp. 35–40, 2013.

[70] G. C. Blackhart, J. A. Minnix, and J. P. Kline, "Can EEG asymmetry patterns predict future development of anxiety and depression: A preliminary study," *Biol. Psychol.*, vol. 72, no. 1, pp. 46–50, 2006.

[71] M. D. Sacchet, G. Prasad, L. C. Foland-Ross, P. M. Thompson, and I. H. Gotlib, "Elucidating brain connectivity networks in major depressive disorder using classification-based scoring," in *Proc. IEEE Int. Symp. Biomed. Imag.*, Apr./May 2014, pp. 246–249.